Ocean Circulation Modeling for Aquatic Dispersion of Liquid Radioactive Effluents from Nuclear Power Plants

Y.G. Chung, G.B. Lee, S.Y. Bang
Korea Electric Power Research Institute
103-16 Munji-Dong, Yuseong-Gu, Daejeon 305-380
Korea

S.B. Choi, S.U. Lee
Korea Hydro & Nuclear Power Co., LTD
167 Samseong-Dong, Gangnam-Gu, Seoul 135-791
Korea

J.H. Yoon
Research Institute of Applied Physics, Kyushu University
6-1 Kasuga-kouen, Kasuga, Fukuoka, 816-8580
Japan

S.Y. Nam, H.R. Lee
GeoSystem Research Corporation
306 Hanlim Human Town, 1-40 Geumjeong-Dong, Gunpo-City, Gyeonggi-Do 435-050
Korea

ABSTRACT

Recently, three-dimensional models have been used for aquatic dispersion of radioactive effluents in relation to nuclear power plant siting based on the Notice No. 2003-12 "Guideline for investigating and assessing hydrological and aquatic characteristics of nuclear facility site" of the Ministry of Science and Technology (MOST) in Korea. Several nuclear power plants have been under construction or planed, which are Shin-Kori Unit 1 and 2, Shin-Wolsong Unit 1 and 2, and Shin-Ulchin Unit 1 and 2. For assessing the aquatic dispersion of radionuclides released from the above nuclear power plants, it is necessary to know the coastal currents around sites which are affected by circulation of East Sea. In this study, a three dimensional hydrodynamic model for the circulation of the East Sea of Korea has been developed as the first phase, which is based on the RIAMOM (Research Institute of Applied Mechanics' Ocean Model, Kyushu University, Japan). The model uses the primitive equation with hydrostatic approximation, and uses Arakawa-B grid system horizontally and Z-coordinate vertically. Model domain is 126.5°E to 142.5°E of east longitude and 33°N and 52°N of the north latitude. The space of the horizontal grid was 1/12° to longitude and latitude direction and vertical level was divided to 20. This model uses Generalized Arakawa Scheme, Slant Advection, and Mode-Splitting Method. The input data were from JODC (Japan Oceanographic Data Center), KNFRDI(Korea National Fisheries Research and Development Institute), and ECMWF (European Center for Medium-Range Weather Forecasts) . The modeling results are in fairly good agreement with schematic patterns of the surface circulation in the East Sea/Japan Sea. The local current model and aquatic dispersion model of the coastal region will be developed as the second phase. The oceanic dispersion experiments will be also carried out by using ARGO Drifter around a nuclear power plant site.

INTRODUCTION

In Korea, total 20 units of nuclear power plants have been operated at 4 sites - Kori, Ulchin, Wolsong and Younggwang. Several new nuclear power plants have been under construction or planed, which are Shin-Kori Unit 1 and 2, Shin-Wolsong Unit 1 and 2, and Shin-Ulchin Unit 1 and 2.

Recently, three-dimensional models have been used for aquatic dispersion of radioactive effluents in relation to nuclear power plant siting based on the Notice No. 2003-12 "Guideline for investigating and assessing hydrological and aquatic characteristics of nuclear facility site" of the Ministry of Science and Technology (MOST) in Korea. Therefore, KEPRI (Korean Electric Power Research Institute) and KHNP (Korea Hydro & Nuclear Power Co., LTD) have been developed a three-dimensional aquatic dispersion model for radioactive

effluents released from nuclear power plants located at east coast of Korea. For assessing the aquatic dispersion of radioactive effluents from the above new nuclear power plants, it is necessary to know the circulation of the water mass in the East Sea/Japan Sea.
In this study, many models such as MOM, RIAMOM, KEY-POM, MICOM were analyzed through literature surveys [1, 2]. A three dimensional hydrodynamic model for the circulation of the East Sea of Korea has been developed in the first phase, which is based on the RIAMOM (Research Institute of Applied Mechanics' Ocean Model, Kyushu University, Japan).

MODEL DESCRIPTION

Model equation

The RIAMOM model assumes hydrostatic balance with Boussinesq approximation, and solves the three-dimensional, non-linear, primitive external and internal model equations on Arakawa-B system[2, 3]. The internal model equations of the model in the spherical coordinates are:

$$\frac{1}{Rcos\Phi}\frac{\partial u}{\partial \lambda}+\frac{1}{Rcos\Phi}\frac{\partial}{\partial \Phi}(\nu\cos\Phi)+\frac{\partial w}{\partial x}=0 \quad \text{(Eq. 1)}$$

$$\frac{\partial u}{\partial t}+L(u)-\frac{uvtan\Phi}{R}-fv=-\frac{1}{\rho_0 Rcos\Phi}\frac{\partial P}{\partial \lambda}+\frac{\partial}{\partial z}A_\nu\frac{\partial u}{\partial z}+A_h\nabla^2 u-\frac{u}{R^2\cos^2\Phi}-\frac{2\sin\Phi}{R^2 coc^2\Phi}\frac{\partial \nu}{\partial \lambda} \quad \text{(Eq. 2)}$$

$$\frac{\partial v}{\partial t}+L(v)-\frac{u^2\tan\Phi}{R}-fu=-\frac{1}{\rho_0 R}\frac{\partial P}{\partial \Phi}+\frac{\partial}{\partial z}A_\nu\frac{\partial v}{\partial z}+A_h\nabla^2 v-\frac{v}{R^2\cos^2\Phi}-\frac{2\sin\Phi}{R^2 coc^2\Phi}\frac{\partial u}{\partial \lambda} \quad \text{(Eq. 3)}$$

$$\frac{\partial P}{\partial z}=-\rho g \quad \text{(Eq. 4)}$$

$$\frac{\partial T}{\partial t}+L(T)=\frac{\partial}{\partial z}K_v\frac{\partial T}{\partial z}+K_h\nabla^2 T \quad \text{(Eq. 5)}$$

$$\frac{\partial S}{\partial t}+L(S)=\frac{\partial}{\partial z}K_v\frac{\partial S}{\partial z}+K_h\nabla^2 S \quad \text{(Eq. 6)}$$

Where t is the time, λ is the longitude, φ is the latitude, R is the radius of the earth, f is the Coriolis parameter (=2Ωsinφ, Ω is the earth's angular velocity), g is the gravitational acceleration, P is the pressure, ρ is the density of seawater, ρ0 is the reference density, u, v and w are the zonal, meridional and vertical components of the currents, respectively, T and S represent seawater temperature and salinity, respectively, and Kv and Kh denote the coefficients of the vertical and horizontal eddy diffusivities, respectively.

The advection and Laplacian operators denoted by L and nabla □2, respectively, are defined as:

$$L(\mu)=\frac{1}{Rcos\Phi}\frac{\partial}{\partial \lambda}(u\lambda)+\frac{1}{Rcos\Phi}\frac{\partial}{\partial \Phi}(v\mu\cos\Phi)+\frac{\partial}{\partial z}(w\mu) \quad \text{(Eq. 7)}$$

$$\nabla^2\mu=\frac{1}{R^2\cos^2\Phi}\frac{\partial^2\mu}{\partial\lambda^2}+\frac{1}{R^2\cos\Phi}\frac{\partial}{\partial\Phi}(\cos\Phi\frac{\partial\mu}{\partial\Phi}) \quad \text{(Eq. 8)}$$

The UNESCO equation of state adapted by Mellor is used to calculate the density [4]. The external model equations are derived by integrating equations (1) to (3) in the vertical [5].

Model Domain and Grid

The model domain and basic grid configuration taken in this study are identical the those of Kim [6]. The model area covers the sea region from 126.5oE to 142.5 oE in longitude and from 33.0 oN to 52.0 oN in latitude. The inflow regions of the model are Jeju Strait and the west coast of Kyushu and the outflow regions are Tsugaru Strait and Soya Strait (Fig. 1). Both of the latitudinal and longitudinal grid intervals are chosen as 1/12o. The number of vertical layers is a total 20 variable levels as illustrated at Table I. The depth field shown in Fig. 1 has been extracted from the ETOPO5 global depth data [7]. The model area is divided to 8 sectors to use parallel computing method.

Eddy Viscosity and Diffusivity

In this model, the vertical eddy viscosity (Av) and diffusivity (Kv) coefficients are 1.0 cm2/sec and 0.1 cm2/sec, respectively. The Horizontal eddy viscosity (Ah) and diffusivity(Kh) coefficients are set to values about six orders higher than the vertical counterparts. The eddy viscosity values are same as those used by Kim [6].

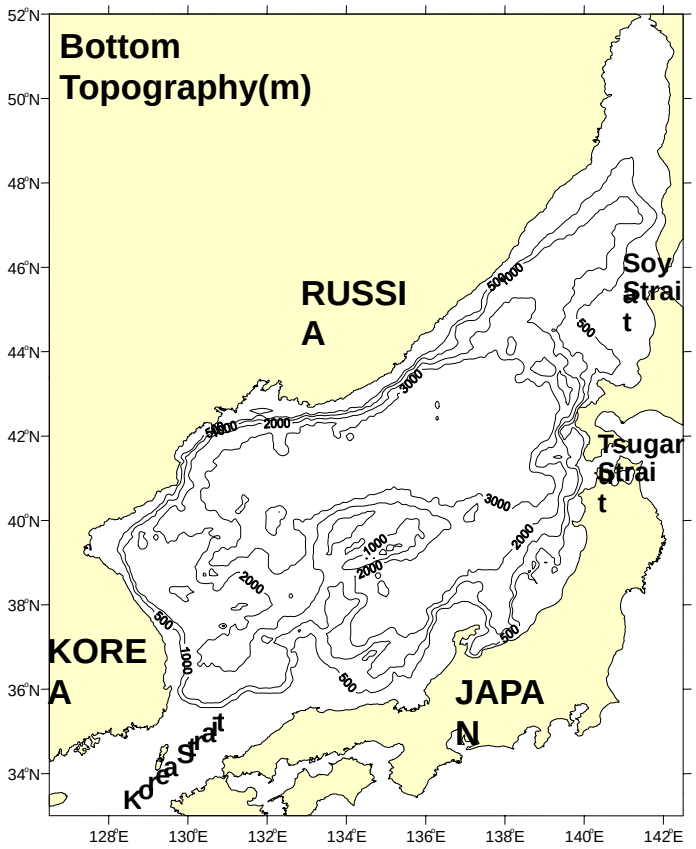

Fig. 1. Model domain with bottom topography

Table I. Vertical Layers of the Model

Vertical levels	interval of layer(in meters)	Depth of Water(in meters)
1	5	2.5
2	7.5	8.75
3	10	17.5
4	12.5	28.75
5	15	42.5
6 ~ 8	20	100
9	40	130
10 ~ 12	50	275
13 ~ 14	100	450
15 ~ 16	250	875
17 ~ 18	500	1750
19	800	2400
20	1050	3325

Volume Transports at the Inflow and Outflows

At the inflow region, we have specified seasonally varying volume transport of the Tsushima Warm Current (TWC)that has been prepared on the basis of regular(six time a week) monitoring of the flow variation across the Korea/Tsushima Strait from February, 1997 to August, 2002 using an ADCP mounted on a ferry [8]. The average volume transport of the TWC is 2.65 Sv(1 Sv=106 m3/sec) and 1.54 Sv in east channel , 1.11 Sv in west channel of The TWC with strong seasonal variability. The variation of the observed volume transport shows two maximum in March to June and other maximum in September to November. The minimum of the volume transport occurs around the middle of February, reaching about 1.5 Sv~2.0 Sv.

The outgoing volume transport through the Tsugaru Strait is fixed as 1.4 Sv throughout the calculation, taking into account the ADCP observation of Shikama [9]. The volume flowing out through the Soya Strait is then adjusted to maintain the mass balance within the domain. The volume transports are equally distributed to each grid along the open boundaries. The external component of velocity consistent with the in flow and outflow boundaries can be calculated from the volume transports and the section of the grids.

Along with the volume transports, temperature and salinity are imposed at the inflow boundary based on the monthly mean observations by the Fisheries Research and Development Agency of Korea [10]. The near-surface temperature reaches a maximum in August and a minimum in March showing a variation of about 12.6oC, while the near-bottom temperature reaches a maximum near November and a minimum in March showing a variation of about 4 oC to 4.5oC. The near-surface salinity reaches a maximum in March and a minimum in August showing a variation of about 2.8 psu to 3.0 psu, while the near-bottom salinity reaches a maximum in March and a minimum in October or November showing a variation of about 0.1 psu to 0.25 psu. Based on the observations, monthly mean values over a year are prepared in advance and are repeatedly used for the multi-year integration.

The internal component of velocity consistent with the inflow boundaries is calculated from the prescribed temperature and salinity distribution along the boundaries based on the assumption of the thermal wind relation. No gradient condition has been applied at the outflow boundary. The velocity component tangential to the open boundaries is set at zero. The no-slip, insulating, and impermeable boundary conditions are applied along the lateral land boundaries.

Sea Surface and Sea Bottom Boundary Conditions

The boundary conditions for momentum at the sea surface and bottom are:

$$A_v \frac{\partial(u,v)}{\partial z} = \frac{(\tau_{w\lambda}, \tau_{w\Phi})}{\rho_0} \quad \text{z=0}$$

$$A_v \frac{\partial(u,v)}{\partial z} = \frac{(\tau_{b\lambda}, \tau_{b\Phi})}{\rho_0} \quad \text{z=H} \qquad \text{(Eq. 9)}$$

where $\tau_{w\lambda}$, $\tau_{b\lambda}$ and $\tau_{w\varphi}$, $\tau_{b\varphi}$ are zonal and meridional components of shearing stress, respectively. Subscripts in the equation (9) denote the depth levels whose derivatives are taken. At the sea surface, the monthly mean wind stresses of the re-analyzed ECMWF data are imposed and, at the sea floor, the usual quadratic bottom friction ($\rho_0 C_d (u_b, v_b)\sqrt{u_b^2 + v_b^2}$), where u_b and v_b are near-bottom velocities, respectively) is used along with the drag coefficient (C_d) of 0.0026. The monthly mean wind stresses are calculated from the daily wind stress data with a horizontal resolution of 0.5625° in both longitude and latitude from January 1992 to December 2000.

While the bottom boundary conditions for temperature and salinity are given as a zero flux in line with that of the seabed, a thermohaline forcing is used at the sea surface as:

$$K_v \frac{\partial T}{\partial z} = \frac{Q_T}{\rho_0 C_p}, \qquad K_v \frac{\partial S}{\partial z} = Q_S \qquad \text{z=0} \qquad \text{(Eq. 10)}$$

where Q_T and Q_s are the heat and salt fluxes, and C_P is the specific heat of seawater at constant pressure. The surface flux of heat (Q_T) is given as a Bernier type suggested by Barnier *et al*. [11], which is expressed as:

$$Q_T = Q^*_T + \rho C_p \Delta z_1 (T^*_s - T_s)/\tau \qquad \text{(Eq. 11)}$$

where Q^*_T is the net heat flux with a horizontal resolution of 0.5625° from ECMWF data. T^*_s is the sea surface

temperature obtained from Korea Oceanographic Data Center (KODC) and Japan Oceanographic Data Center (JODC) and Ts is the simulated water temperature at the first level below the sea surface. $\rho$is density of sea water, Δz_1 is the interval of the first level, and τ is restoring time scale (30 days)

A Newtonian type restoring boundary condition is applied to the salt flux at the sea surface with the constant damping time of 10 days. That is,

$$Q_s = \gamma^{-1}(S_s - S_1) \qquad \text{(Eq. 11)}$$

where γ is the restoring time scale (10 days), S1 the simulated water salinity at the first level below the sea surface, Ss the observed sea surface salinity. For Ss, we have used the long-term monthly mean sea surface salinity data constructed by Kim [6] on the basis of the Japan Oceanographic Data Center (JODC), the Fisheries Research and Development Agency of Korea (FRDAK) and the Far Eastern Hydrometeorological Institute of Russia (FEHMI).

The sea surface temperature and salinity data were from JODC (Japan Oceanographic Data Center), KNFRDI(Korea National Fisheries Research and Development Institute), and wind data were from ECMWF (European Center for Medium-Range Weather Forecasts).

RESULTS AND DISCUSSION

Comparison between Model Results and GDEM data

In comparison of the two model results (MOM, RIAMOM), we have used the U.S Navy's monthly mead temperature and salinity data. The source of GDEM is the U.S. Navy's Master Oceanography Observation Data Set (MOODS), which is a composite dataset based on observations from various sources from 1930-97 [12]. Fig. 2 shows horizontally averaged, annual-mean vertical profiles of temperature and salinity from MOM (dotted line), RIAMOM (dashed line) and the GDEM data (solid line). We can see that the two model results agree well with each other. Considerable differences between the model results and the GDEM data are however seemingly apparent. It is noted that the difference between the model results and the GDEM data gradually increases below 50 m; more diffusive forms of thermocline and halocline have been simulated than noted in the GDEM data.

The difference is about 2oC in temperature and 0.07-0.1 psu in salinity below 300 m.

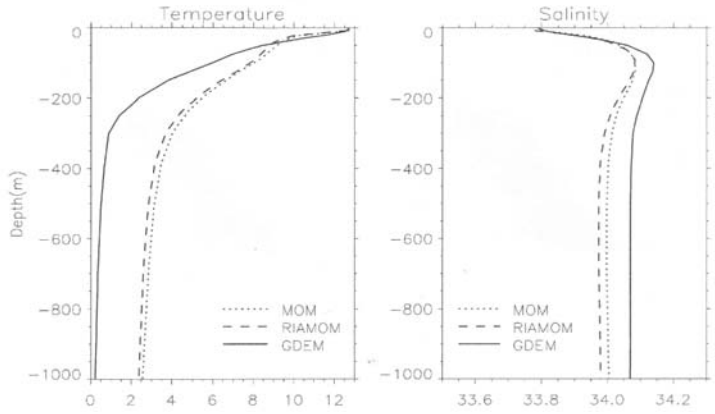

Fig. 2. Vertical profiles of temperature (left) and salinity (right), calculated from the time-averaged and area-averaged values over model domain and 1 year. Solid, dotted, and dashed lines are for the GDEM Data, MOM, and RIAMOM, respectively.

Flow fields comparison

The flow fields at the bottom levels of the models are of value for the comparison of model results. Fig. 3 displays the snapshots of the flow fields at bottom levels of the models in the middle of February. It is worthwhile noting that MOM produces a noisy pattern with grid-scale disturbances along the Russian coast where the steep bottom slope exists. This might attribute to neglecting the slant advection along the steep bottom topography in MOM as shown by Ishizaki and Motoi [13] and Webb [14]. In proposing a new advection scheme, Ishizaki and Motoi [13] noted the importance of including the diagonally upward/downward

momentum advection (so called the slant advection) along the bottom slope and an enstropy conserving advection scheme (so called the generalized Arakawa scheme) for the horizontal advection of momentum. According to their results, the most prominent difference in the velocity field appears along the steep coastal sea regions; the old Cox code run using the simple centered approximation of advective terms produces a noisy pattern with grid-scale disturbances, while the new scheme shows rectified flows. In addition, the noisy pattern does not appear in the two-dimensional barotropic flow. For these reasons, they concluded that the grid-scale disturbances appeared in the old Cox code run might be suppressed by means of slant advection, as also discussed by Webb [14]. It appears that the noisy pattern enhances the horizontal diffusion, smoothing out more effectively the velocity field in MOM than in RIAMOM. Consequently, RIAMOM produces more rectified flows on the coastal region, for example, narrower and stronger NKCC/LCC, than MOM.

Model results illustrated at Fig. 4 appear to effectively reproduce the distinct features of circulation in the East Sea/Japan Sea such as the first branch of the TWC (the so-called NB) flowing along the Japanese coast, the EKWC (East Korean Warm Current) flowing northward along the Korean coast, and the NKCC/LCC(North Korean Cold Current/Liman Cold Current) flowing southwestward along the Korean/Russian coast. Overall patterns of circulation are in fairly good agreement with schematic patterns of the surface circulation in the East Sea/Japan Sea which were previously suggested in several papers ([15], [16], [17]). We can also see that the EKWC is significantly stronger in August than in February, while the NKCC/LCC becomes pronounced in February due to the strong winter monsoons. The EKWC breaks away from the Korean coast near 38oN in the results.

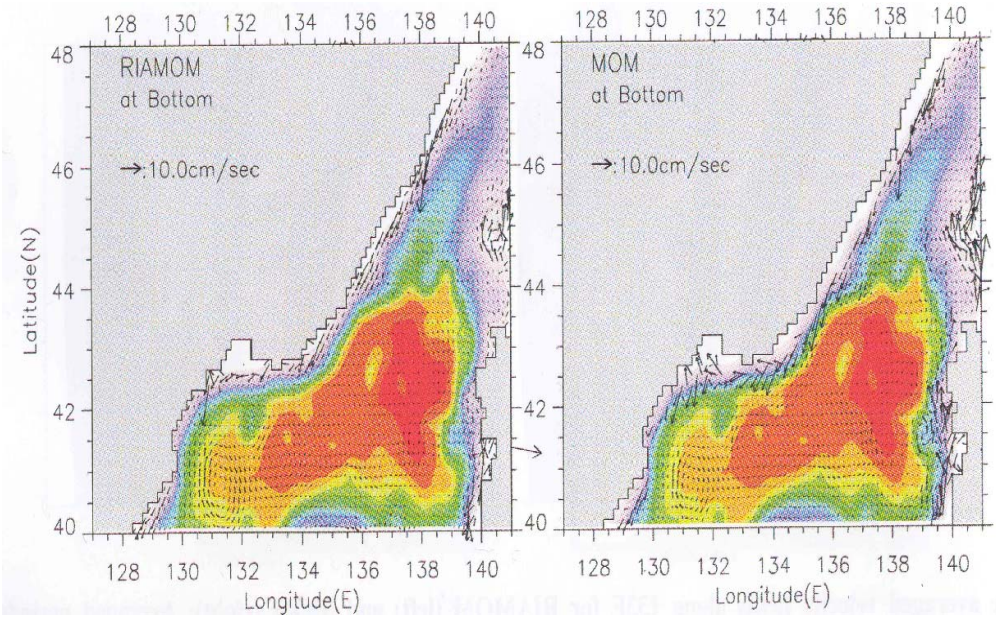

Fig. 3. Instantaneous velocity fields at bottom levels of RIAMOM (left) and MOM (right) in the middle of February. Colors denote bottom topography.

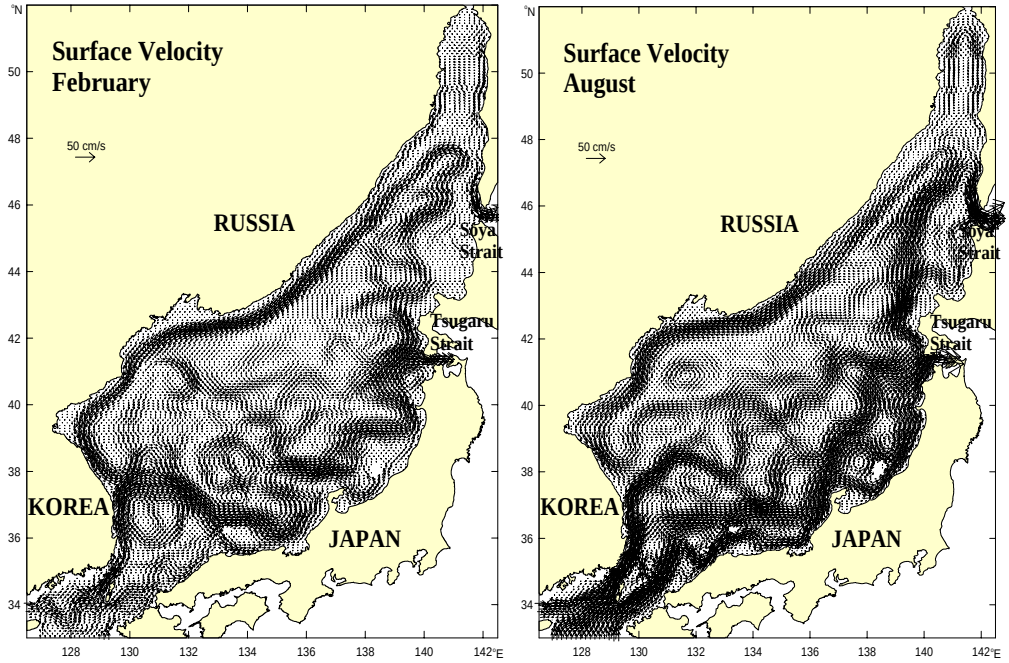

Fig. 4. Monthly averaged surface velocity fields in February and August

CONCLUSION AND FURTHER STUDY

For assessing aquatic dispersion of radioactive effluents in relation to nuclear power plant siting, a three dimensional hydrodynamic model for the circulation of the East Sea of Korea has been developed as the first phase of this study. The model is based on the RIAMOM (Research Institute of Applied Mechanics' Ocean Model, Kyushu University, Japan).

RIAMOM results agree well with MOM results and GDEM data. In bottom flow field comparison between RIAMOM and MOM, It appears that the noisy pattern enhances the horizontal diffusion, smoothing out more effectivety the velocity field in MOM than in RIAMOM. Consequently, RIAMOM produces more rectified flows on the coastal region because RIAMOM includes slant advection scheme.

In the second phase of this study, the local current models and aquatic dispersion models for the coastal regions within a 50-mile radius of the nuclear power plants will be developed by using one-way nesting method. Furthermore, the oceanic dispersion experiments will be also carried out by using ARGO Drifter around a nuclear power plant site at east coast of Korea(Ulchin, Wolsong, Kori).

REFERENCES

1. Kim, K.J., Y.H. Seung, and M.S. Sulk. (2001). POM/MICOM inter-comparison in modeling the East Sea circulation. Ocean and Polar Res., 23(2), 161-172.
2. Lee, H.J., J.H. Yoon, Hideyuki Kawamura, and H.W. Kang. (2003). Comparison of RIAMOM and MOM in modeling the East Sea/Japan Sea circulation. Ocean and Polar Res., 25(3) 287-302.
3. Lee, H.C. and J.H. Yoon. (1994) On the free surface OGCM. 225-226. In: proceeding of Fall Meeting of Japan Oceanographical Society.
4. Mellor, G.L (1996). An equation of state for numerical models of ocean and esteries. J. Atmos. Ocean Technol., 8, 609-611.
5. Lee, H.C. (1996). A numerical simulation for the water masses and circulations of the Yellow Sea and the East China Sea, Japan. Ph. D. Thesis, Kyushu Univ., 150p.
6. Kim. C.H. (1996). A numerical experiment study on the circulation of the East Sea(Japan Sea), Japan. Ph. D. Thesis., Kyushu Univ., 151p.

7. NCAR. (1989). NCAR ASCII Version of ETOPO5 earth surface elevation. Data Support Section, NCAR.
8. Takikawa, T., J.H. Yoon, and K.D. Cho. (2003), Tidal currents in the Tsushima Straits estimated from ADCP data by ferryboat. J. Oceanogr., 59, 37-47.
9. Shikama, N. (1994). Variation of volume transport in the Tsugaru Strait measured by bottom-mounted ADCP. Kaiyo Monthly, 815-818
10. National Fisheries Research and Development Agency of Korea. (1986). Mean Oceanographic Charts of the Adjacent seas of Korea. NFRDA, Busan. 186p
11. Barnier B., L. Siefried, and P. Marchesiello. (1995). Thermal forcing for a global ocean circulation model using a three-year climatology of ECMWF analyses. Journal of Marine Systems, 6, 363-380.
12. Chu, P.C., J. Lan, and C. Fan. (2001). Japan Sea thermohaline structure and circulation. Part: Climatology. J. Phys. Oceanogr., 31, 244-270.
13. Ishizaki, H. and T. Motoi. (1999). Reevaluation of the Takano- Oonishi scheme for momentum advection on bottom relief in ocean models. J. Atmos. Ocean Technol., 16, 1994-2010.
14. Webb, D.J. (1995). The vertical advection of momentum in Bryan-Cox-Semtner ocean general circulation models. J. Phys. Oceanogr., 25, 3186-3195.
15. Yarchin, V.G. (1980). Study state of the Japan Sea. p. 46-61. In: Problems of Oceanography, ed. by V. Pokudov. Hydrometeoizdat, Leningrad. (In Russian)
16. Kim, C.H. and J.H. Yoon. (1996). Modeling of the winddriven circulation in the Japan Sea using a reduced gravity model. J. Oceanogr., 52, 359-373.
17. Kim, K., K.Y. Kim, D.H. Min, Y. Volkov, J.H. Yoon, and M. Takematus. (2001). Warming and structural changes in the East (Japan) Sea: a clue to future changes in global oceans?. Geophys, Res. Lett., 28, 3293-3296